Sigma J Eng & Nat Sci 38 (4), 2020, 1837-1848

Sigma Journal of Engineering and Natural Sciences
Sigma Mühendislik ve Fen Bilimleri Dergisi

Research Article

THE ATMOSPHERIC TRANSPORTED DESERT DUST OVER SANLIURFA (TURKEY) AND ITS STRUCTURAL PROPERTIES

Tuba RASTGELDİ DOGAN*[1], Serife Pinar YALCIN[2]

[1]*Dept. of Environmental Eng., Harran University, SANLIURFA;* ORCID: 0000-0002-8246-388X
[2]*Department of Physics, Harran University,SANLIURFA;* ORCID: 0000-0002-9791-5623

Received: 16.08.2020 Revised: 02.12.2020 Accepted: 03.12.2020

ABSTRACT

In this study, atmospheric dust samples were collected via Partisol 2025 ID device working in EPA mode by using PM_{10} (Particulate matter less than 10 microns) filter during 2016-2017 from Sanliurfa, Turkey. The arrival direction and source detection of atmospheric dust was determined by the MODIS satellite view and HYSPLIT model. The structure of the samples was characterized by XRD (X-Ray Diffraction), SEM (Scanning Electron Microscopy) combined with EDX (Energy Dispersive X-ray) and FTIR (Fourier Transformed Infrared Spectrum). Results show that the major phases observed in the XRD spectrum of the samples are calcite, dolomite, gibbsite, anorthite, and sodium borate hydroxide. The compositions of dust samples were found to be Ca, Si, Al, Na, and Mg in a higher ratio than other elements via SEM-EDX analysis. Further, this study reveals the variability of PM morphological and elemental composition on different days at locations and highlighted the different probable sources associated with them.
Keywords: Atmospheric transported desert dust, PM, HYSPLIT model, XRD, SEM-EDX.

1. INTRODUCTION

Dust particles in deserts called particulate matter can be carried far away through winds caused by differential pressure. Atmospheric dust transport contamination causes considerable harm to the environment as well as human health as it involves air particulate matter which is a blend of organic and inorganic contaminants [1]. Even though the main resources are dry areas, due to the air circulation around the world, mineral particles are carried over long ranges. As an example, Saharan dust, which generates approximately 2x108 tons of aerosols every year and is transported on the Atlantic Ocean towards the Mediterranean Sea beside the south part of Europe, is the most important natural resource of PM [2-4]. The harsh dust-storms commonly in Middle East & Africa contribute to carrying a great amount of air contamination, especially to the environmental particulate matter contamination [5-7]. Moreover, they also serve as an effective platform to scavenge or convert gases. Typically, atmospheric dust transport stems from resources such as soils, neighboring desert settings, industrial contaminants, traffic jams, unfinished fuel combustion in house heating, physical plants, and vehicle exhausts [8]. Soil dust stands for the main components of the atmospheric dust transport specimens. Qualification of the atmospheric

* Corresponding Author: e-mail: trastgeldi@harran.edu.tr, tel: (414) 318 30 00 / 1262

dust transport specimens in terms of physics, chemistry, and mineralogy is crucial to figure out the effect of atmospheric dust transport both on the environment and human well-being. Dust sources, no matter how big or stro ng they are, maybe correlated with topographically low altitudes placed in dry districts that receive yearly precipitation below 200-250 mm such as Iran, Iraq, Jordan, the Southern part of Turkey, Saudi Arabia, Kuwait, and Syria. In addition to this, the Sahara is known to be the biggest sole origin of the atmospheric dust [9].

Located in Southeastern Anatolia Region with a Syria border, Sanlıurfa is a significant city due to air flows, through which PM (Particulate Matter) sized dust is transported from large deserts such as Sahara, Syria, and Iran and enters the country at various times. Numerous studies have been conducted to determine the physical and chemical features of dust in mass as well as single dust particles (i.e. size distribution, particle morphology, chemical/mineral composition) to determine the environmental interactions of dust [10-13]. Weather conditions can be affected by the atmospheric particulates, particularly the ones dislocated through dust storms [14-17]. Atmospheric dust can change both mineral components and morphology of solid particulates [18], the geological and geomorphological structure of the place as well as the form and destination of the wind [19,20]. This fact is vital for comprehending the characteristics and the origin of the dust. Jeong and Achterberg investigated the chemical and mineralogical structure of clay minerals within Asian and Saharan dust. According to them, the analysis of dust in mass through X-ray diffraction shows that Saharan dust is more abundant in clay minerals, whereas Asian dust contains more chlorite [21,22], have found out in another research, on the mineralogical properties and core features of singular fine particles of Sahara-originated dust, that the mineralogical properties and core features of individual particles of Sahara-originated dust particles include main ferrous minerals (i.e) illite–smectite series clay minerals and iron (hydro)oxides [22]. The present study is aimed to investigate and compare the structural properties by XRD, SEM-EDX, and FTIR methods of the Syrian, Saharan, and Arabian Peninsula atmospheric dust particles collected from Sanliurfa, Turkey.

2. METHODS

Partisol 2025ID sampler was located to the Harran University, Osmanbey Campus, Sanlıurfa (37.17 ^{0}N and 39.00 ^{0}E), Turkey, and it was used to collect atmospheric particles. Two samples of PM_{10} were collected every day. The device makes 16.7 L/min traction. Sample intakes were 1.4 m high on the instrument to prevent suspended particles near to the ground surface during strong winds. The special filters in 47 mm diameter were used that could both trap atmospheric particulates and continue to function during the suction process and under very dusty conditions. In the period from March to May, collapsing dust was collected from deserts that affected the region through TS2544 collapsing dust collection device located in the same place.

X-ray diffraction patterns of the samples were obtained by using a Rigaku D-max 2000 X-Ray diffractometer with CuKα radiation (λ = 1.5406 Å) at 40 kV and 30mA. The diffraction pattern was scanned with a step size of 0.02 at a 10–60^{o} angle range. The mineral phase, which is the characteristic diffraction peak of each sample, was determined using Jade 7.0 software and the ICDD database. To characterize shapes and sizes of atmospheric dust samples, SEM (ZEIS EVO 50 scanning electron microscope) with magnification ranging from 500 to 5000 times interfaced with an energy dispersive X-ray analysis system (EDX) and Si(Li) detectors were used. Samples were put on a carbon disk and coated with gold for 5 minutes. FT-IR spectrum of HR100 samples was taken using the ATR method between 600-4000 cm^{-1} via Shimadzu IRTracer-100 Fourier transform infrared spectrophotometer.

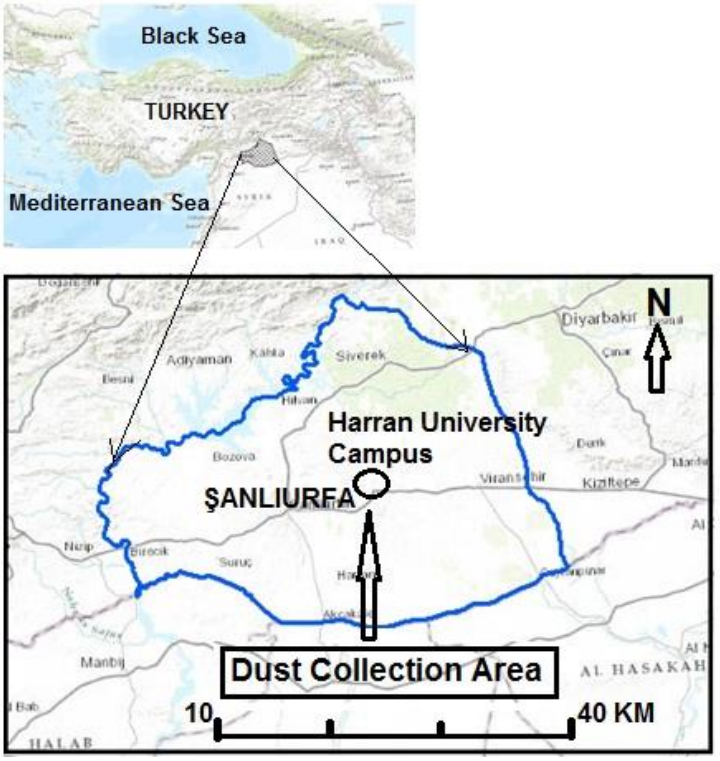

Figure 1. Study area where dust collection device was set up.

3. RESULTS AND DISCUSSION

3.1. Samples

The diagnosis of physical-chemical features and mineralogical structure of atmospheric particulates resources is highly significant as the content of the particulate matter varies depending on the source regions [23-26]. In many studies, dust transport has been detected using MODIS and HYSPLIT. For example, [27], used MODIS to determine the transport of dust in the Cyprus region in her study in 2016. Sanliurfa province is affected by the surrounding deserts as a result of air movements.

The information of the studied atmospheric dust samples in this study is given in Table 1. As shown in Fig.2(a) and 2(b), the source region is Sahara. The Sahara is known to carry billions of desert dust every year with atmospheric transport to different countries of the world by air movements. Fig. 2(c) and 2(d) came from Syria, which is a border country.

Fig.2 (e) and 2 (f) show how air quality is affected by the deserts in the Arabian Peninsula. As these deserts have different sources, they differ in an element and chemical content.

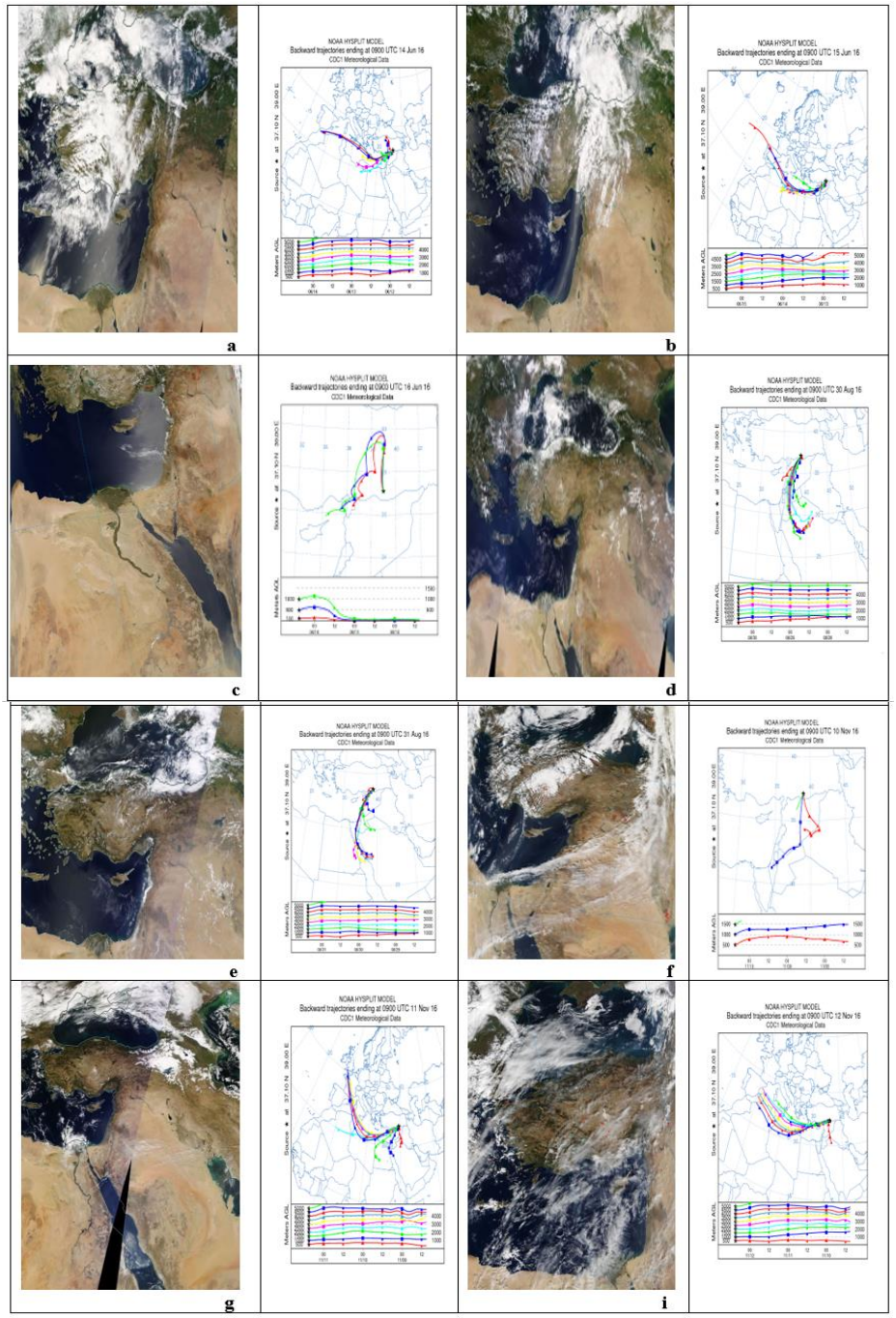

Figure 2. MODIS and HYSPLIT satellite information (a) HC4, (b) HC5, (c) HC6, (d) HC48, (e) HC49, (f) HC66, (g) HC67, (i) HC68

Table 1. MODIS and HYSPLIT Satellite information of the samples

Date	Sample Code	$PM_{2.5}$($\mu g\ m^{-3}$)	PM_{10}($\mu g\ m^{-3}$)	Arrival Direction
14 June 2016	HC4	609,72	1012,08	Sahara
15 June 2016	HC5	968,98	1211,25	Sahara
16 June 2016	HC6	972,66	1214,32	Sahara
30 August 2016	HC48	344,91	604,17	Syria
31 August 2016	HC49	344,44	653,33	Syria
10 November 2016	HC66	304,52	653,21	Arab Peninsula
11 November 2016	HC67	316,67	660,42	Arab Peninsula
12 November 2016	HC68	301,39	561,67	Arab Peninsula
March-April-May 2016	HC100	1500,10	2100,75	Sahara, Syria, Arab Peninsula

3.2. XRD

Figure 3 illustrates the XRD diffraction patterns of 10 atmospheric dust samples (HC4, HC5, HC6, HC48, HC49, HC50, HC66, HC67, HC68, and HC100). The mineral compositions of the samples determined through XRD are given in Table 2. As seen in the table, the major phases were found to be calcite ($CaCO_3$) [JCPDF file 01-072-1650 and 1651, 99-000-0548], dolomite ($CaMg(CO_3)_2$) [JCPDF file 01-079-1346], gibbsite ($Al(OH)_3$) [JCPDF file 01-076-1782 and 01-070-2038], anorthite ($(Ca_{0.94}Na_{0.06})(Al_{1.94}Si_{2.06}O_8)$) [JCPDF file 01-084-0750], sodium borate hydroxide ($Na_2B_4O_6(OH)_2$) [JCPDF file 01-070-0789], ammonium aluminum fluoride hydrate ($(NH_4)_2AlF_5.H_2O$) [JCPDF file 00-042-0689], quartz (SiO_2) [JCPDF file 99-000-3084] and Jasmundite [JCPDF file 01-074-0745]. The main components were calcium carbonate as calcite ($CaCO_3$) and dolomite ($CaMg\ (CO_3)_2$), silicon dioxide or quartz (SiO_2), aluminosilicates gypsum ($CaSO_4.2H_2O$) structure as compatible with literature data in the studied samples [28,29]. The main phases were found to include Al (aluminum), Si (silicon), Ca (calcium), and F (fluoro). Some new formations such as Jasmundite were also observed in the XRD pattern. Some researchers report that the samples can be affected mainly by natural processes such as physical and chemical weathering, which could vary from one site to another, and maybe traffic (exhaust from local vehicles), exhausts of residential central heating, and industrial activity [30].

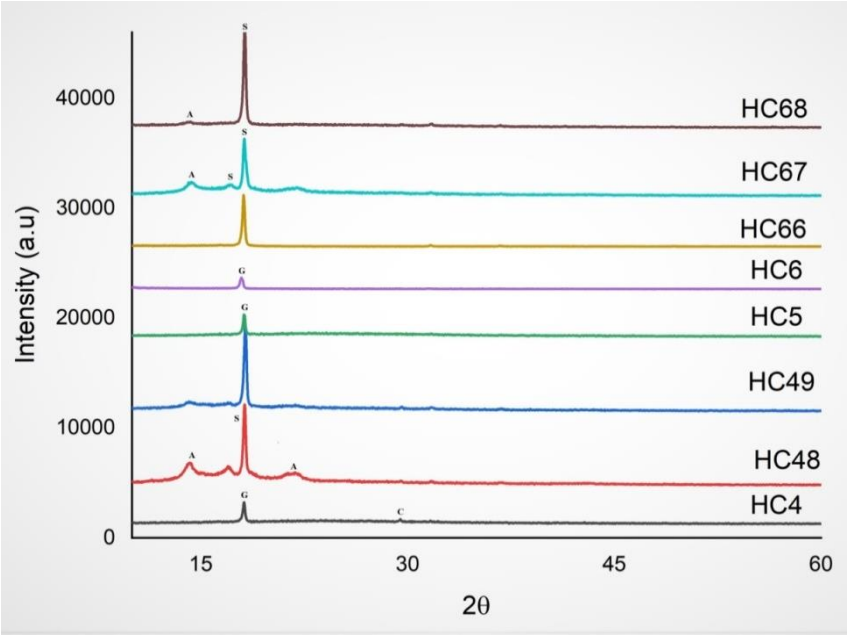

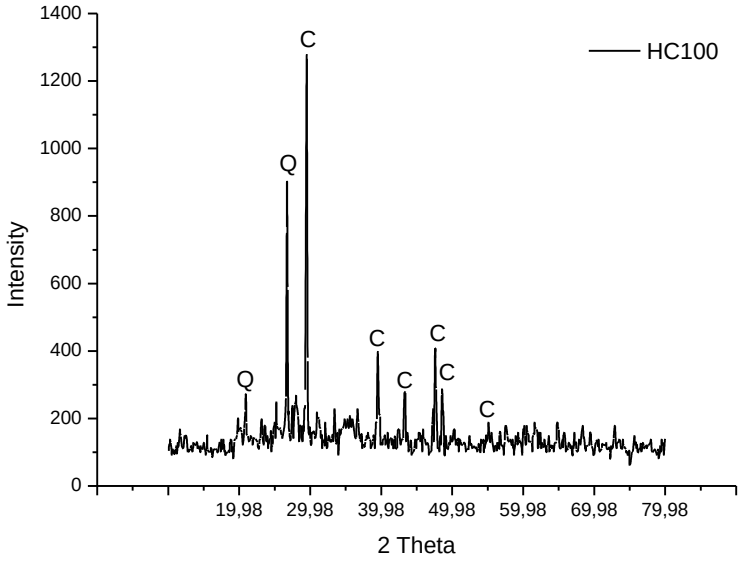

Figure 3. XRD pattern of the atmospheric dust sample, Here Q: Quartz G: Gibbsite, S: Sodium Borate Hydroxide, C: Calcite; D: Dolomite; A: Anorthite

Table 2. The mineral phase of the samples.

Dust Samples	Phase	Pdf number	Phase	Pdf number	Phase	Pdf number
HC4	Gibbsite	01-070-2038	Calcite	01-072-1651	-	-
HC5	Gibbsite	01-076-1782	Dolomite	01-079-1346	-	-
HC6	Jasmundite	01-074-0745	Ammonium Aluminium Fluoride Hydrate	00-042-0689	-	-
HC48	Sodium Borate Hydroxide	01-070-0789	Calcite	01-072-1650	Anorthite	01-078-1629
HC49	Sodium Borate Hydroxide	01-070-0789	Calcite	01-072-1650	Anorthite	01-078-1629
HC50	Jasmundite	01-074-0745	Ammonium Aluminium Fluoride Hydrate	00-042-0689	-	-
HC66	Jasmundite	01-074-0745	Ammonium Aluminium Fluoride Hydrate	00-042-0689	-	-
HC67	Sodium Borate Hydroxide	01-070-0789	Calcite	01-072-1650	Anorthite	01-078-1629
HC68	Sodium Borate Hydroxide	01-070-0789	Calcite	01-072-1650	Anorthite	01-078-1629
HR100	Quartz	99-000-3084	Calcite	98-000-0548	-	-

The dust obtained from the Saharan Desert consists mostly of the gibbsite and calcite mineral phase. It also includes small quantities of dolomite due to abundant clay minerals and carbonates [31]. Aluminosilicate clay minerals form over half of mineral dust from Africa and Asia [32]. Calcite is known to exist due to the lack of rainfall in the surrounding areas and it is produced in atmospheric dust transport samples [33]. Compared to the Sahara Desert, the atmospheric dust samples from Arabian and Syrian deserts have higher sodium borate hydroxide and anorthite. [34], reports that sodium and silica components are subject to rapid fluctuations from one sample locality to another. The source of borate minerals is presumably volcanic thermal springs genetically related to basalt flows that underlie the shale [35].

3.3. SEM

The composition of mineral dust was also determined by using scanning electron microscopy (SEM) combined with energy dispersive X-ray microanalysis (EDX). Element analyses show that these samples contain Ca, Si, Al, Na, and Mg element in a higher ratio than other elements (Table 3). HC48 and HC68 have higher calcium rates while HC5 and HC49 include higher Si elements compared to other samples. The aluminum element observed in SEM-EDX analyses in HC4 shows the gibbsite structure in XRD data analyses. Higher Si and Ca ratio in the element ratio table of HC49 is anorthite structure in the XRD pattern. HC4 and HC5 have different element content although they were taken from the Saharan desert. The high Si and Ca rate attracts attention in the microstructure observation of the HR100 sample similar to the XRD pattern of

this sample [36], expresses that local differences in the mineralogical composition of the undifferentiated source rocks and weathering conditions can affect the characteristics of samples.

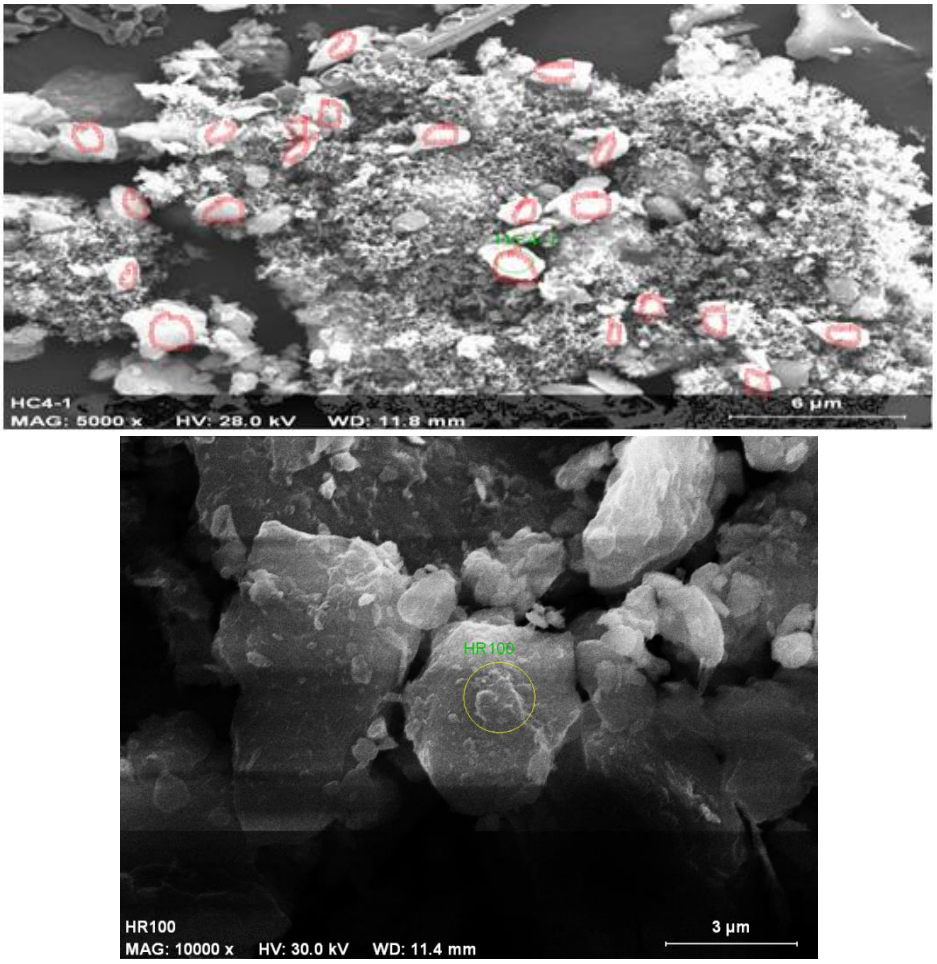

Figure 4. SEM image of HC4 and HR100 samples.

Table 3. The elemental composition of atmospheric dust samples.

Atom/Element	Si	Al	Fe	Mg	Ca	K	Na	O	C	Ti	Cl	Cu
HC4	10.91	5.55	2.20	2.78	1.58	0.97	1.43	72.67	-	-	-	-
HC5	0.91	0.91	0.16	1.17	22.61	-	2.11	54.79	14.76	-	-	-
HC48	4.44	2.63	0.49	2.42	54.47	0.25	-	32.64	0.4	-	-	-
HC49	15.11	5.73	2.07	3.26	7.48	1.39	0.29	61.54	1.72	0.34	0.18	-
HC67	5.75	2.28	0.37	1.83	29.36	0.22	2.15	54.15	1.88	-	0.36	-
HC68	1.15	0.55	0.10	0.48	53.35	-	-	41.27	0.71	-	-	0.32
HR100	14.96	6.33	1.78	3.92	18.01	0.51	0.06	54.12	-	0.17	-	-

3.4. FTIR

The FTIR spectrum of the HR100 sample can be seen in Figure 5. This spectrum contains a mixed structure consisting of quartz and calcite. The silicate minerals are a primary concern because of their relative abundance and importance. Quartz (SiO_2) is common and invariably present in all the samples. The Si-O bonds are the strongest in the silicate structure and can be readily recognized in the infrared spectra of such minerals by very strong bands in the region 900-1100 cm^{-1} is due to stretching as well as less intense bands in the 400-800 cm^{-1} region are due to bending [37]. The quartz mineral in the samples were detected with bands at 618 cm^{-1}, 778 cm^{-1}, 800 cm^{-1}, 816cm^{-1} and 1014,5 cm^{-1}. Calcite form was observed at 1440 cm^{-1}, 1642 cm^{-1}, 1743 cm^{-1}, 1797 cm^{-1}, 2854 cm^{-1} and 2926 cm^{-1}. Radulescu et al. expresses that these bands exhibit $SO4^{2-}$ (612-617 cm^{-1}), NO_3^- (820-840 cm^{-1}, and 1350-1359 cm^{-1}), SiO^{-4} (777-794 cm^{-1} and 1035 cm^{-1}), CO_3^{2-} (871-885 cm^{-1} and 1450 cm^{-1}), NH_4^+ (1410-1412 cm^{-1}), carbonyl group, C = O (1640-1645 cm^{-1}) and aliphatic carbon, C-H (1455 and 2919-2937 cm^{-1}) [38].

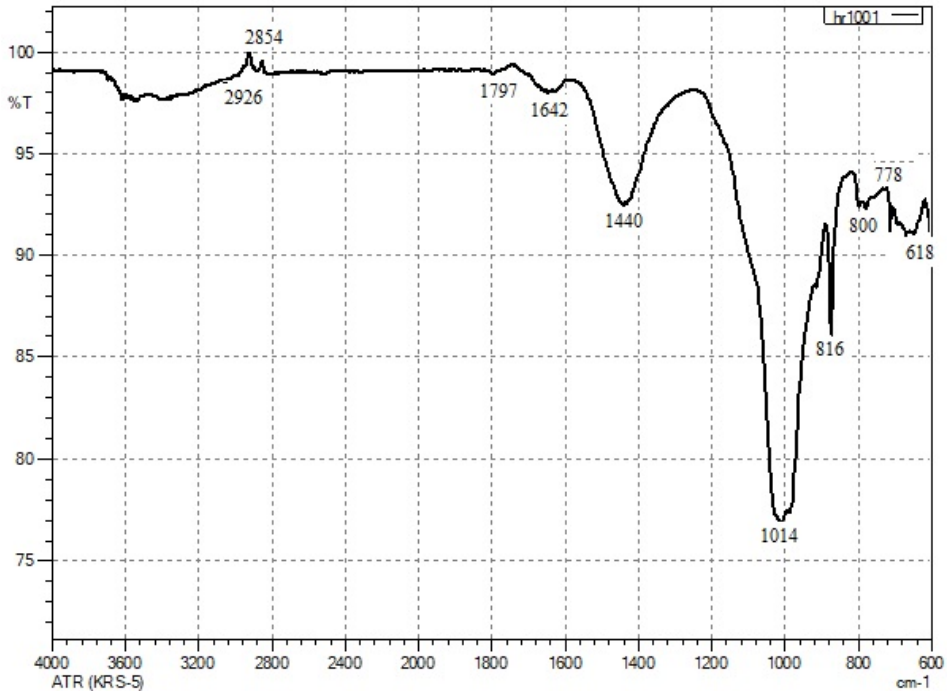

Figure 5. FTIR spectrum of HR100 sample

4. CONCLUSION

The present study represents the structural characterization of atmospheric dust transported to the southern region of Turkey, Sanliurfa. Six samples were collected from different locations and at different times. Based on XRD measurements, the major phases found in the studied samples were observed to be calcite ($CaCO_3$), dolomite ($CaMg(CO_3)_2$), gibbsite ($Al(OH)_3$), anorthite ($(Ca_{94}Na_{06})(A_{l1.94}Si_{2\cdot06}O_8)$), and sodium borate hydroxide ($Na_2B_4O_6(OH)_2$). SEM-EDX measurements showed good agreement with XRD results. FTIR spectrum of HR100 showed mixed structure formed from calcite and quartz.

Acknowledgments

The authors thank Harran University Scientific and Technological Research Center (HUBTAM) for XRD and SEM-EDX measurements.

REFERENCES

[1] Gonzalez-Martin, C., Coronado-Alvarez, N.M., Teigell-Perez, N., Diaz-Solano, R., Exposito, F.J., Diaz, J.P., Griffin, D.W. & Valladares, B. (2018). Analysis of the Impact of African Dust Storms on the Presence of Enteric Viruses in the Atmosphere in Tenerife, *Spain Aerosol Air Qual. Res*.18.1863–1873.

[2] Mitsakou, C., Kallos, G., Papantoniou, N., Spyrou, C., Solomos, S., Astitha, M. & Housiadas, C. (2008). Saharan dust levels in Greece and received inhalation doses. *Atmos. Chem. Phys.* 8(23),7181-7192.

[3] Kallos, G., Astitha, M., Katsafados, P. & Spyrou, C. (2007). Long-range transport of anthropogenically and naturally produced particulate matter in the Mediterranean and North Atlantic: Current state of knowledge. *J. Appl. Meteor. Climatol*. 46,81230-1251.

[4] Querol, X., Alastuey, A., Ruiz, C.R., Artiñano, B., Hansson, H. C., Harrison, R. M. & Straehl, P. (2004). Speciation and origin of PM10 and PM2.5 in selected European cities. *Atmos. Environ.* 38(38), 6547-6555.

[5] Akbari, B., Tavandashti, M.P. & Zandrahimi, M. (2011). Particle size characterization of nanoparticles–a practicalapproach. *Iran. J. Mater. Sci. Eng*. 8. 4

[6] Saliba, N., Massoud, R., Shihadeh, A.L., Roumié, M., Youness, M., Gerard, J. and Saliba, & N. A. (2011). Intraurban variability of PM10 and PM2.5 in an Eastern Mediterranean city. *Atmos. Res.*101(4),893-901.

[7] Al-Awadh, M.S. (2013). U.S. Patent No. 8,424,573. Washington, DC: U.S. *Patent and Trademark Office.*

[8] Balal, O., Eisa, S. & Asgar, S. (2018). Characterızatıon And Morphologıcal Analysıs Of Aerosols In Tehran Traffic Zone. *J.Air Poll.Health*.3,1. 9- 16

[9] Aleksandropoulou, V. & Lazaridis, M. (2013). Identification of the influence of African dust on PM10 concentrations at the Athens air quality monitoring network during the period 2001–2010. *Aerosol Air Qual Res*. 13.1492-1503.

[10] Shaltout, A.A., Welz, B. & Castilho, I.N.B. (2013). Determinations of Sb and Mo in Cairo's dust using high-resolution continuum source graphite furnace atomic absorption spectrometry and direct solid sample analysis. *Atmos Environ*. 81, 18–24

[11] Alghamdi, I. G., Hussain, I. I., Alghamdi, M. S., Dohal, A. A., Almalki, S. S. & El-Sheemy, M. A. (2015). The incidence rate of thyroid cancer among women in Saudi Arabia: an observational descriptive epidemiological analysis of data from Saudi Cancer Registry 2001–2008. *J Imiigr Minor Healt*. 17.3.638-643.

[12] Alharbi, F.H. & Kais, S. (2015). Theoretical limits of photovoltaics efficiency and possible improvements by intuitive approaches learned from photosynthesis and quantum coherence. *Renew Sust Energ Rev*. 43.1073-1089.

[13] Habeebullah, T. M., Munir, S., Mohammed, A. M., Morsy, E. A., Rehan, M. & Ali, K. (2016): Analysing PM2.5 and its association with PM10 and meteorology in the arid climate of Makkah, Saudi Arabia. *Aerosol Air Qual. Res*. 17.453-464.

[14] Buseck, P.R. & Posfai, M. (1999). Airborne minerals and related aerosol particles: Effects on climate and the environment. *Proc. Natl. Acad. Sci*. 96(7), 3372-3379.

[15] Prospero, J.M. (1999). Assessing the impact of advected African dust on air quality and health in the eastern United States; Human and Ecological Risk Assessment. An International Journal. 5(3), 471-479.

[16] Clarke, A.D., Collins, W.G., Rasch, P.J., Kapustin, V.N., Moore, K., Howell, S. & Fuelberg, H.E. (2001). Dust and pollution transport on global scales: aerosol measurements and model predictions. *J. Geophys*. Res. 106.32555-32569.

[17] Bishop, J.B.K., Davis, R.E. & Sherman, J.T. (2002). Robotic observations of dust storm enhancement of carbon biomass in the North Pacific. *Science*. 298. 817-821

[18] Singer, A., Ganor, E., Dultz, S. & Fischer, W. (2003). Dust deposition over the Dead Sea. *J. Arid Environ*. 53. 41-59.

[19] Engelbrecht, J.P., McDonald, E.V., Gillies, J.A., Jayanty, R.K.M., Casuccio, G. and Gertler, A.W. (2009): Characterizing mineral dusts and other aerosols from the Middle East—Part 1: ambient sampling. *Inhal Toxıcol*. 21,297–326.

[20] Zarasvandi, A., Carranza, E. J. M., Moore, F. & Rastmanesh, F. (2011). Spatio-temporal occurrences and mineralogical–geochemical characteristics of airborne dusts in Khuzestan Province (southwestern Iran). *J Geochem Explor*. 111,(3). 138-151.

[21] Jeong, G.Y. & Achterberg, E.P. (2014). Chemistry and mineralogy of clay minerals in Asian and Saharan dusts and the implications for iron supply to the oceans. *Atmos. Chem. Phys*. 14. 12415–12428.

[22] Jeong, G.Y., Park, M.Y., Kandler, K., Nousiainen, T. & Kemppinen, O. (2016). Mineralogical properties and internal structures of individual fine particles of Saharan dust. *Atmos. Chem. Phys.* 16,19 . 12397-12410.

[23] Bergametti, G., Gomes, L., Coudé-Gaussen, G., Rognon, P., & Le Coustumer, M.N. (1989). African dust observed over Canary Islands: Source-regions identification and transport pattern for some summer situations. *J. Geophys. Res. Atmos*. 94(12),14855-14864.

[24] Merrill, J., Arnold, E., Leinen, M. & Weaver, C. (1994). Mineralogy of aeolian dust reaching the North Pacific Ocean: 2. Relationship of mineral assemblages to atmospheric transport patterns. *J. Geophys*. Res. 99, 21025-21032.

[25] Davis, B.L. & Guo, J. (2000). Airborne particulate study in five cities of China. *Atmos. Environ.*34. 2703-2711.

[26] Ganor, E., Deutsch, Y. and Foner, H.A. (2000): Mineralogical composition and sources of airborne setting particles on Lake Kinner et (the Sea of Galilee), Palestine. *Water Air Soil Poll*. 118.245-262.

[27] Mamouri, R. E., Ansmann, A., Nisantzi, A., Solomos, S., Kallos, G. & Hadjimitsis, D. G. (2016). Extreme dust storm over the eastern Mediterranean in September 2015: satellite, lidar, and surface observations in the Cyprus region. *Atmos. Chem. Phys*. 16(21), 13711-13724.

[28] Gonzalez, L.T., Longoria Rodríguez, F.E., Sanchez-Domínguez, M., Leyva-Porras, C., Silva-Vidaurri,L.G., Acuna-Askar, K., Kharisov, B.I., Villarreal Chiu, J.F., Alfaro Barbosa J.M., (2016). Chemical and morphological characterization of TSP and PM2.5 by SEM-EDS, XPS and XRD collected in the metropolitan area of Monterrey, Mexico. *Atmos Envıron*.143. 249-260.

[29] Shaltout, A.A., Allam M.A., Mostafa, N.Y., & Heiba Z.H. (2016): Spectroscopic Characterization of Dust-Fall Samples Collected from Greater Cairo, Egypt. *Arch Environ Contam Toxicol*. 70, 544–555.

[30] Godelitsas, A., Nastos, P., Mertzimekis T.J., Toli, K., Simon, R., & Göttlicher, J., (2011). A microscopic and Synchrotron-based characterization of urban particulate matter (PM10–PM2.5 and PM2.5) from Athens atmosphere, Greece. *Nucl Instrum Methods*.3077–3081.

[31] Jeong, G.Y. (2008). Bulk and single-particle mineralogy of Asian dust and a comparison with its source soils. *J. Geophys. Res. Atmos*.113 D2

[32] Freedman, M.A. (2015). Potential sites for ice nucleation on aluminosilicate clay minerals and related materials. *J. Phys. Chem. Lett*. 6,19.3850-3858.

[33] Shaltout, A.A., Allam, M.A., Mostafa N.Y. & Heiba Z.K. (2016). Spectroscopic Characterization of Dust-Fall Samples Collected from Greater Cairo, Egypt, Arch Environ Con Tox. 70,544–555.

[34] Rashki, A., Eriksson, P.G., Rautenbach, C.D.W., Kaskaoutis, D.G., Grote, W. & Dykstra, J. (2013). Assessment of chemical and mineralogical characteristics of airborne dust in the Sistan region, Iran. *Chemosphere*. 90,2. 227-236.

[35] Dibblee, T.W. (1967): Areal geology of the western Mojave Desert, California.

[36] Prakash, J.P., Stenchikov, G., Tao, W., Yapici, T., Warsama, B. & Engelbrecht, J.P. (2016): Arabian Red Sea coastal soils as potential mineral dust sources. *Atmos. Chem. Phys*. 16,18: 11991-12004.

[37] Senthil Kumar, R., & Rajkumar P. (2014). Characterization of minerals in air dust particles in the state of Tamilnadu, India through FTIR, XRD and SEM analyses. *Infrared Phys Techn*. 67, 30–41.

[38] Radulescu, C., Stihi, C., Iordach, J., Dunea, S., & Dulama, I.D. (2017). Characterization of Urban Atmospheric PM2.5 by ATR-FTIR, ICP-MS and SEM-EDS Techniques. *Rev Chım.* 68:4.